Study of the Characteristics of Battery Packs in Electric Vehicles With Parallel-Connected Lithium-Ion Battery Cells

Xianzhi Gong, *Student Member, IEEE*, Rui Xiong, *Member, IEEE*, and Chunting Chris Mi, *Fellow, IEEE*

***Abstract*—This paper studies the characteristics of battery packs with parallel-connected lithium-ion battery (LiB) cells. To investigate the influence of the cell inconsistency problem in parallel-connected cells, a group of different degraded LiB cells were selected to build various battery packs and test them using a battery test bench. The physical model was developed to simulate the operation of the parallel-connected packs. The experimental results and simulation indicate that, with different degraded cells in parallel, there could be capacity loss and large difference in discharge current, which may cause further accelerated degradation and a more serious inconsistency problem.**

***Index Terms*—Battery, degradation, electric vehicle, lithium-ion battery, modeling, state of charge, state of health.**

I. Introduction

CURRENTLY, lithium-ion batteries (LiBs) are considered as one of the major viable energy-storage solutions for electric vehicles (EVs) and plug-in hybrid EVs (PHEVs). The battery pack provides power and energy to drive the vehicle, as shown in Fig. 1. Typically, the power demands can be up to 30–120 kW. To satisfy the operation voltage and traction power demands, battery packs have to be made with hundreds of cells connected in series or parallel [1], [2]. For example, the battery pack of a Nissan Leaf EV consists of 192 cells, with two cells in parallel; for a Chevrolet Volt PHEV, the battery pack is made of 288 cells, with three cells in parallel, to meet the 350-V system voltage requirement [11], [12].

For battery packs with series-connected cells, it is feasible to monitor and control each cell, in order to avoid overcharge and overdischarge, by applying passive or active balancing modules [3]–[5]. However, there are tremendous technological challenges on how to avoid the adverse effects of cell inconsistency with parallel-connected cells in battery packs (referred to as parallel-connected packs in this paper) and how to prolong the life of both the packs and the cells.

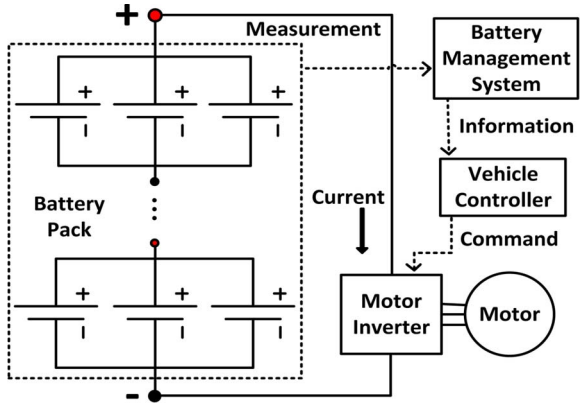

Fig. 1. Typical battery-powered EV drive system.

For onboard battery management systems (BMSs), it is hard to measure the current of each cell in parallel-connected battery packs because it is impractical and costly to add additional current sensors to a BMS to monitor individual cell current [6]. As a result, the behaviors of each single cell in parallel are hard to monitor and manage by the BMS. A variety of researches have been conducted to provide the accurate model-based management for LiB cells [2] and battery packs with series-connected cells [3]. However, few studies about parallel-connected battery packs have been done.

This paper focuses on the study of the characteristics of parallel-connected battery packs. A number of experiments are conducted, in order to investigate the cell inconsistency problem and its influence over parallel-connected packs for EV and PHEV applications. Based on the analysis of the experimental results, it is possible to develop a model for the battery pack as well as the battery state estimation algorithm. Section II of this paper describes the background of the battery modeling and the cell inconsistency problem. The experimental procedures and test bench setup are described in Section III. Section IV presents the experimental results and the proposed model with simulation and discussion. The conclusion is summarized in Section V.

II. Battery Cell Inconsistency Problem

A. Battery Background

The electrical behavior of batteries is similar to a voltage source in series with impedances (resistance/capacitance).

Manuscript received March 31, 2014; revised June 3, 2014; accepted July 17, 2014. Date of publication August 6, 2014; date of current version March 17, 2015. Paper 2014-TSC-0182.R1, presented at the 2014 IEEE Applied Power Electronics Conference and Exposition, Fort Worth, TX, USA, March 16–20, and approved for publication in the IEEE TRANSACTIONS ON INDUSTRY APPLICATIONS by the Transportation Systems Committee of the IEEE Industry Applications Society.

X. Gong and C. Mi are with the Department of Electrical and Computer Engineering, University of Michigan-Dearborn, Dearborn, MI 48128 USA (e-mail: xianzhigong@gmail.com; mi@ieee.org).

R. Xiong is with the National Engineering Laboratory for Electric Vehicles, School of Mechanical Engineering, Beijing Institute of Technology, Beijing 100081, China (e-mail: rxiong@bit.edu.cn).

Color versions of one or more of the figures in this paper are available online at http://ieeexplore.ieee.org.

Digital Object Identifier 10.1109/TIA.2014.2345951

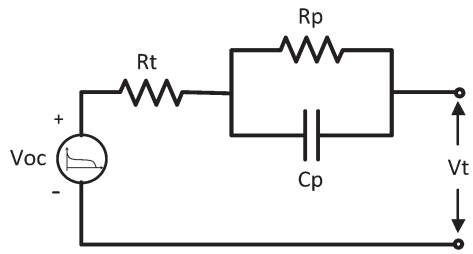

Fig. 2. Equivalent circuit model based on one-order RC network.

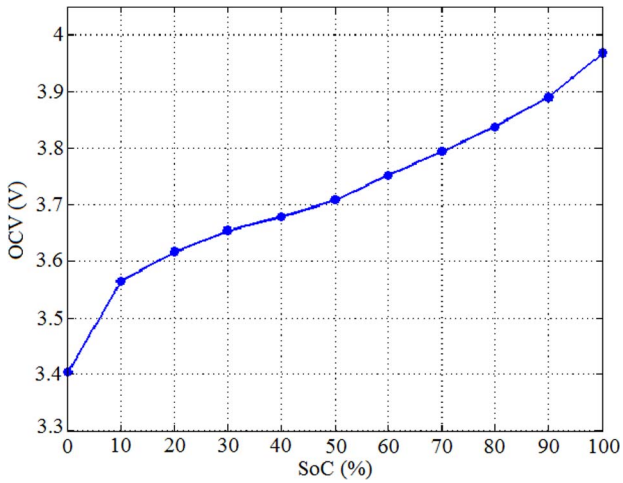

Fig. 3. OCV versus SOC.

However, for EV and PHEV applications, the operation condition and environment of the battery is complex due to the high current, dynamic operation, and regenerative energy. Voltage-source-based battery models are not sufficient to describe and simulate the dynamic behaviors, accurately. In order to solve this problem, the equivalent-circuit-based battery model with RC networks is widely used [10], as shown in Fig. 2.

In this model, $V_{\rm oc}$ denotes the open-circuit voltage (OCV), which is related to the state of charge (SOC) of the battery, as shown in Fig. 3. R_t represents the ohmic resistance. R_p and C_p represent the polarization effect of the battery. These internal parameters are not directly measurable and highly depend on other variables such as SOC and temperature.

B. Cell Inconsistency Problem

The cell inconsistency problem in battery packs reduces the performance and operation efficiency. Once many cells are assembled into a battery pack, the performance of the battery pack cannot be evaluated through adding all single cells together. The reason is that, in the battery pack, the worst cell determines the whole battery pack performance, as shown in Fig. 4. To ensure the battery packs in safety, the BMSs use the lowest and highest SOC of single cells to determine the SOC of the whole battery pack during discharging and charging. Poor cells are more likely to appear severe polarization and generate more heat, which cause the accelerated degradation [10]. As battery packs' service time and cycles increase, the cell inconsistency problem will become worse.

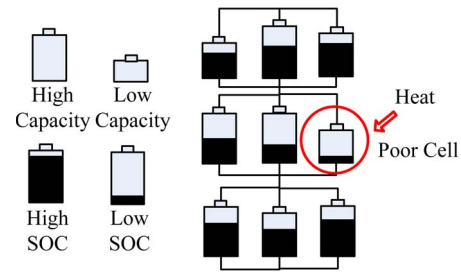

Fig. 4. Battery inconsistency problem in the pack.

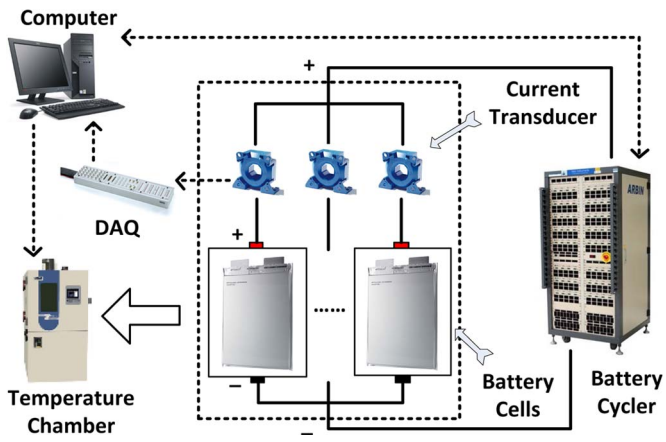

Fig. 5. Battery test bench.

There are various factors that can cause the cell inconsistency problem. In the manufacturing process of battery, the manufacture technique fault, impurity in chemical materials, and human operation errors could result in initial capacity and characteristics difference. Different operating conditions and environments, such as temperature and current rates, may cause different degradation rates and then make the cell inconsistency problem worse.

It is possible to improve the manufacturing process and quality control to solve the problem of initial difference. For normal operation, high-efficiency battery-balancing systems are able to improve the performance and prolong the lifetime of battery packs at some level [4]. However, how to solve the battery cell inconsistency problem completely remains as a tough challenge.

III. Test Bench and Experimental Tests

In order to investigate the characteristics of different degraded battery cells in parallel-connected packs, a test bench capable of measuring the current of each cell was developed. With this test bench, a number of experimental tests were conducted.

A. Test Bench

The battery test bench is shown in Fig. 5. Several different degraded LiB cells and associated Hall effect current transducers are assembled into parallel-connected packs. These packs are placed in the temperature chamber for environment control. The battery cycler performs charging and discharging to the battery packs. The data acquisition system (DAQ) collects

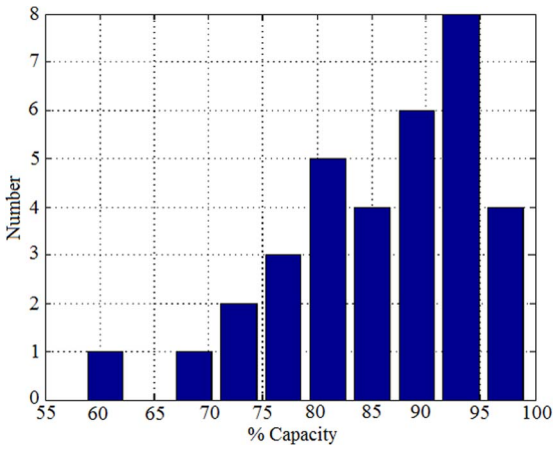

Fig. 6. Cell capacity distribution.

current data from the current transducers and voltage data from the isolation amplifiers for each cell. The connection cables' resistance is measured accurately, in order to eliminate the voltage drops in the tests.

B. Experimental Tests

A group of LiB cells with different degradation levels are selected to conduct the experimental tests. These battery cells have been used in PHEVs for more than two years of real road tests. This battery pack is made with all cells in series, which means all cells share the same current during operation. The nominal voltage of the battery cells is 3.7 V, with a nominal capacity of 32 Ah. The upper cutoff voltage is 4.05 V; the lower cutoff voltage is 3.0 V.

Each cell's present capacity is measured by fully charging and discharging the cell three times with 0.5-C (16-A) current at 25°C. The maximum capacity of these cells is 31.7 Ah, while the minimum one is 18.7 Ah. The capacities are in the range of 58%–99% of the nominal capacity. Most cells remain 80% or higher capacity, as shown in Fig. 6.

A total of 34 cells are assembled into 27 different packs with two, three, and four cells in parallel. The capacity test, hybrid pulse power characterization (HPPC) test, dynamic stress test (DST), urban dynamometer driving schedule (UDDS) test, and federal urban driving schedule (FUDS) test are carried out on these packs. The HPPC test is intended to investigate the dynamic power capability incorporating both discharge and regenerative current pulses. The performance and characteristics can be derived from the HPPC test data [9]. The other tests can be used to simulate the real road driving situations.

IV. Experimental Results and Discussion

With the Capacity, DST, HPPC, UDDS, and FUDS tests, the voltage and current data of each cell are recorded with the 20-Hz sample frequency. Four typical groups are selected to analyze and discuss in this paper.

As shown in Table I, Group 1 and Group 2 each has two cells in parallel, with 0.5- and 10.5-Ah capacity difference, respectively; Group 3 has three cells with 4-Ah capacity difference; Group 4 has four cells with 2.5-Ah capacity difference.

TABLE I
Tested Packs

Group	Cell Number & Capacity			
1	#15 (31.7 Ah)	#19 (31.2 Ah)		
2	#13 (31.7 Ah)	#24 (21.2 Ah)		
3	#06 (22.7 Ah)	#13 (31.7 Ah)	#25 (27.3 Ah)	
4	#05 (28.7 Ah)	#06 (22.8 Ah)	#13 (31.7 Ah)	#27 (26.3 Ah)

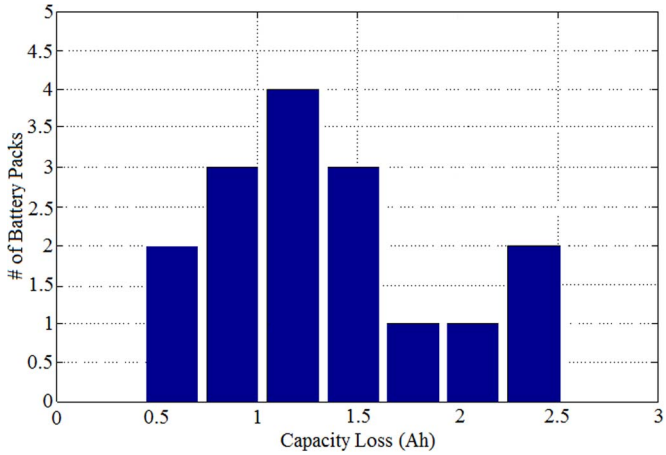

Fig. 7. Capacity loss for battery packs with two cells in parallel.

A. Two Cells Connected in Parallel

Fig. 7 shows the capacity loss of battery packs with two randomly selected cells connected in parallel. The results from capacity tests of these two-cell parallel packs indicate that there are various degrees of capacity loss, ranging from 0.5 Ah to 2.5 Ah, as compared with the sum of individual capacities. These capacity losses could be due to the energy dissipation in the internal resistance and the early reaching of lower voltage limit.

In addition, to verify the dynamic characteristics of the degraded battery cells in electrochemical view, we use electrochemical workstation (ZAHNER IM6) to conduct the electrochemical impedance spectroscopy (EIS) test for Groups 1 and 2. EIS is widely used to investigate the kinetics and determine the degradation level of battery. An excitation signal with small amplitude is applied to the battery, and then, the response is analyzed to get the impedance spectrum. For LiB, it behaves as a nonlinear capacitive load during low frequency. The tendency of the measurement results can express the solid electrolyte interphase diffusion of active material, the electron transportation in the active material particle, and the charge transfer and lithium-ion diffusion in solids [13]. The EIS is an accurate method to determine the degradation level of lithium-ion batteries.

In this EIS test, the frequency range is set from 25 mHz to 1 kHz, with a 10-mV ac excitation signal. The impedance measurements by using Nyquist plots are shown in Fig. 8. Result shows significant differences in comparison with cell #24 and #13, #15, #19. Both imaginary and real parts of the impedance of cell #24 are higher than other cells, which indicates that the degradation level of #24 is highest among these four cells.

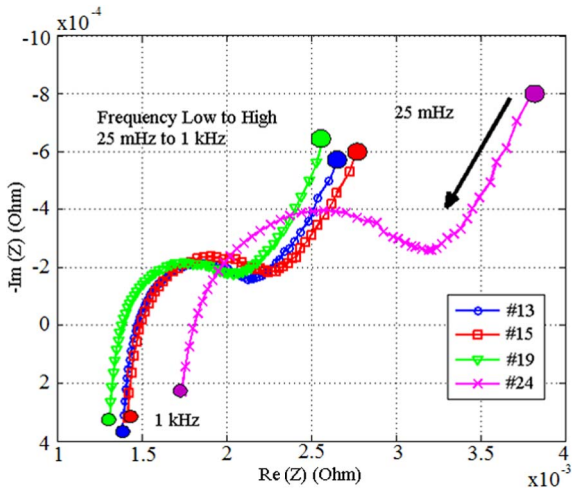

Fig. 8. Impedance test result.

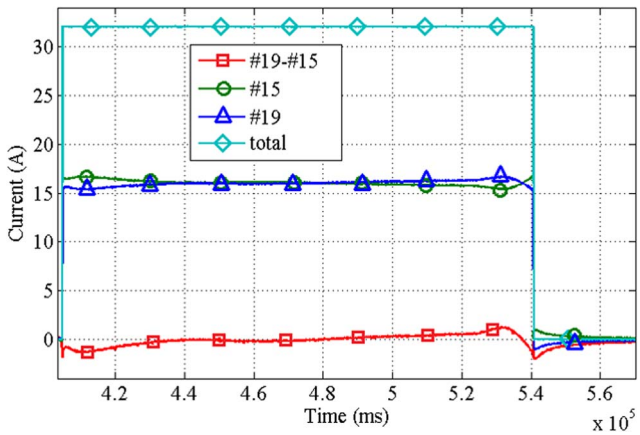

Fig. 9. Cell #19 and #15 discharging current (1C rate: 32 A).

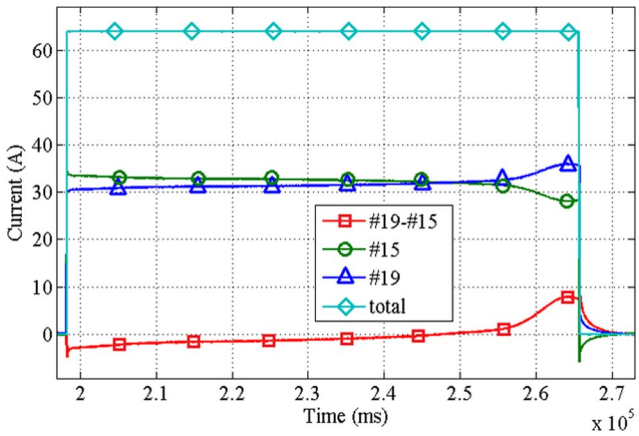

Fig. 10. Cell #19 and #15 discharging current (2C rate: 64 A).

The discharge current of the capacity test (1C/2C discharge) of Groups 1 and 2 are shown in Figs. 9–12. The current difference in Group 1, which is within 2 A, is much smaller than that in Group 2 (20 A). This could be caused by the similarity of internal properties of cells with similar degradation levels. Group-2 current difference becomes larger near the discharging terminal stage. It indicates that the SOC of cell #24 reaches zero earlier than #13, which causes the OCV of cell #24 to drop quickly. Then, #13 is forced to take more current to maintain

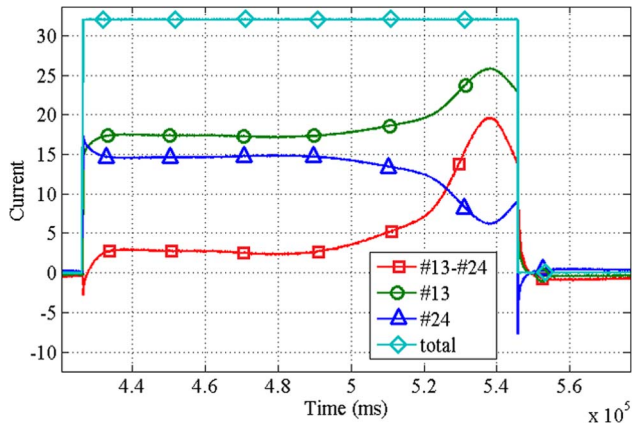

Fig. 11. Cell #24 and #13 discharging current (1C rate: 32 A).

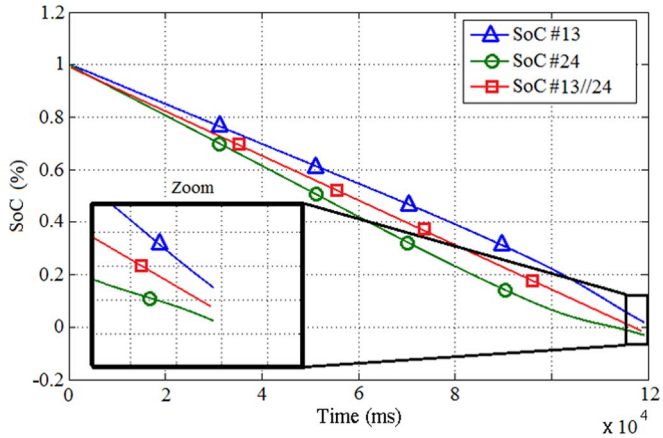

Fig. 12. SOC of cell #24 and #13 discharging current (1C rate: 32 A).

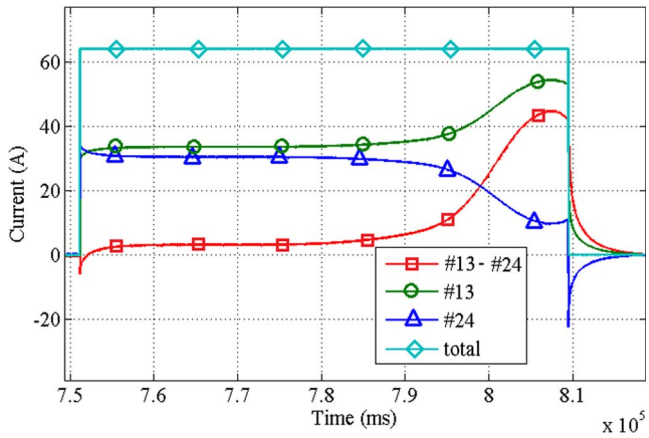

Fig. 13. Cell #24 and #13 discharging current (2C rate: 64 A).

the voltage. Figs. 10–13 show the discharge current of different groups of cells when parallel connected. As shown in Figs. 10 and 13, when the discharging current increases, the current difference also turns to be larger in the end of discharge. The circulating current increases also.

During the discharge process, each cell shares different current due to the difference of internal resistance/polarization effects. Hence, the SOC of each cell changes with different rate, as shown in Fig. 12. At the end of discharge, when the two cells in parallel together reached the lower voltage limit (3 V, 0% SOC for two cells in parallel), the SOCs of each individual cell

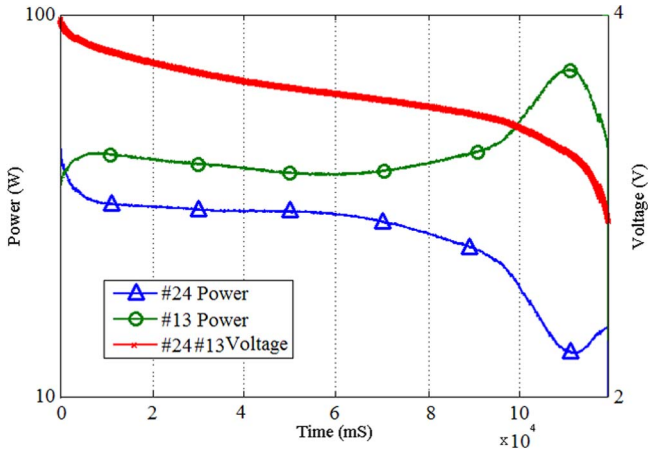

Fig. 14. Cell #24 and #13 discharging power and voltage.

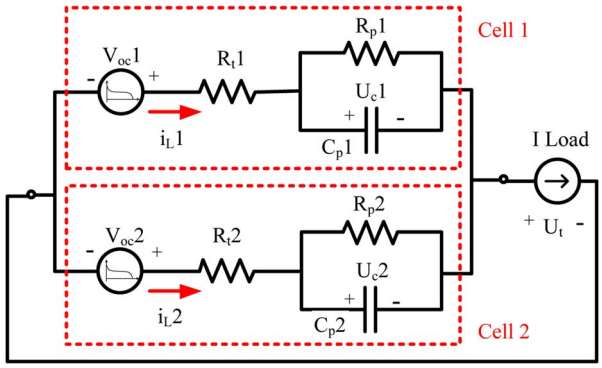

Fig. 15. Lumped parameter model of parallel-connected battery pack.

are not exactly the same, as shown in the zoomed zone. When the discharging is finished, there is a circulating current, which tries to reach the voltage equilibrium condition in each cell due to the different OCV and relaxation effects of these two cells. As a result, one cell in the parallel connection always operates at a higher current and different SOC compared to the other one.

Fig. 14 shows the discharging power and terminal voltage of Group 2. Compared with #24, the output power of #13 is higher during the operation, particularly near the terminal discharging stage. The increasing of current and power leads to higher polarization voltage drop and more heat dissipation. Considering the accelerated degradation effect caused by the high temperature and current [7], cell #13 will degrade more quickly during the operation.

To analyze the detailed characteristics of parallel-connected packs, we build the dynamic lumped parameter model of the battery pack, as shown in Fig. 15.

The pack model includes two RC network-based cell models in parallel, with the load current source. The current variation between i_{L1} and i_{L2} trend mainly depends on the internal parameters such as ohmic resistance R_t, polarization capacitance C_p, resistance R_p, and OCV. These aforementioned parameters are functions of SOC, temperature, and other factors, rather than being a constant [10]. The electrical behavior of the lumped parameter model can be expressed as

$$\begin{cases} \dot{U}_{ck} = -U_{ck}/R_{pk}C_{pk} + i_{Lk}/C_{pk} \\ U_{ck} = \mathrm{OCV}k - U_{ck} - i_{Lk}R_{tk} \\ U_t = \mathrm{OCV}k - U_{ck} - i_{Lk}R_{tk} \end{cases} \quad (k = 1, 2). \qquad (1)$$

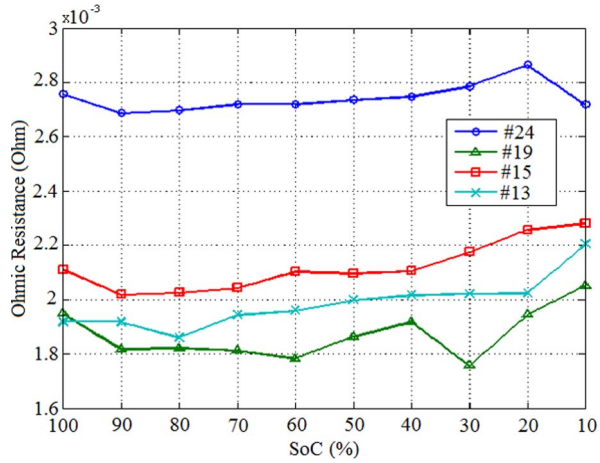

Fig. 16. Ohmic resistance R_t identification result.

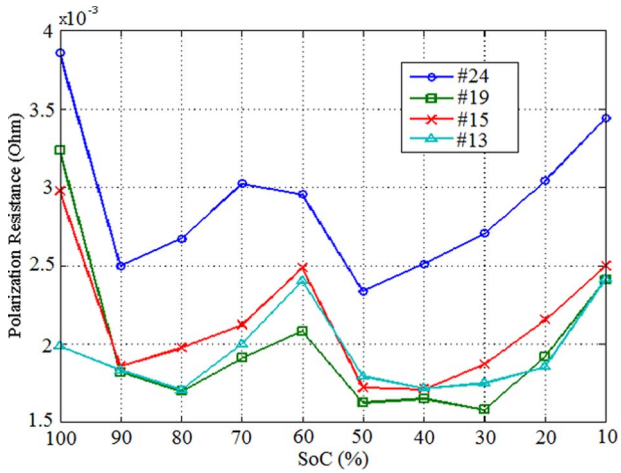

Fig. 17. Polarization resistance R_p identification result.

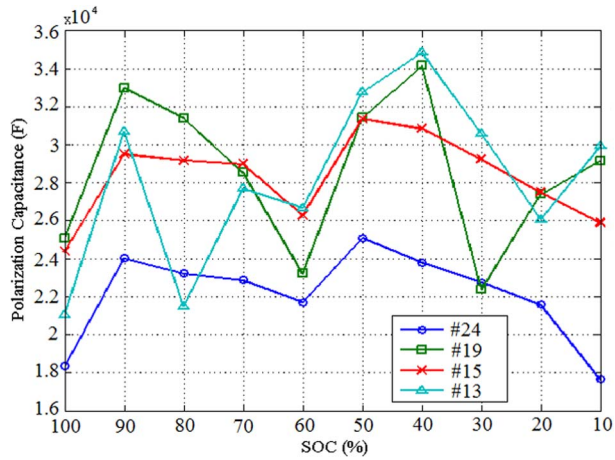

Fig. 18. Polarization capacitance C_p identification result.

In order to obtain the aforementioned SOC-dependent parameters, we use the least mean square method to perform parameter identification based on the HPPC test data. The identification results are shown in Figs. 16–18.

The ohmic resistance difference between #13 and #24 maintains around 0.8 mΩ, in most of the SOC range. While the ohmic resistance difference between cell #19 and #15 is much

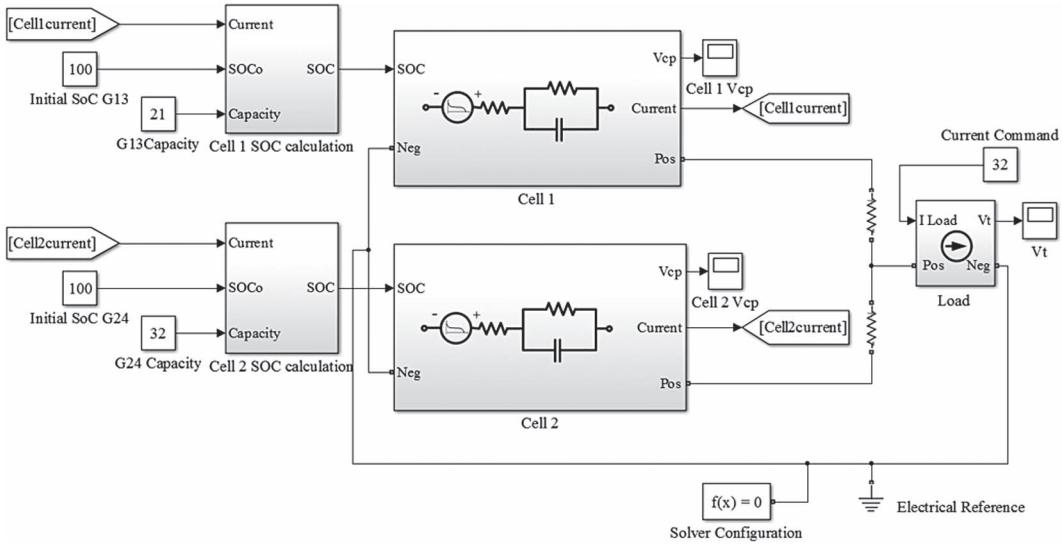

Fig. 19. Battery pack model based on MATLAB/Simulink for two cells in parallel.

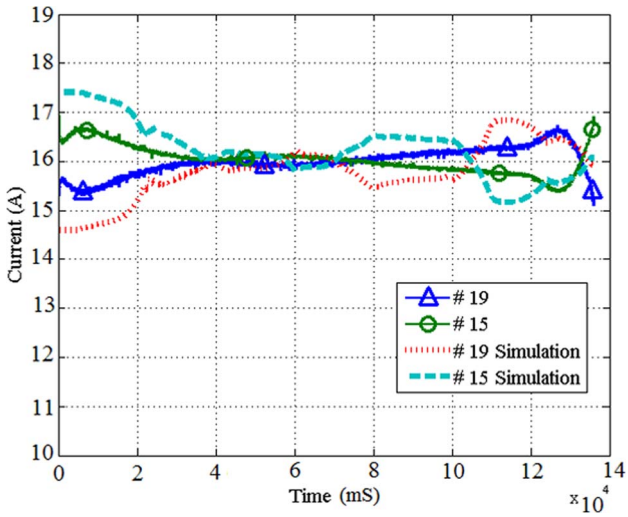

Fig. 20. Cell #15 and #19 simulation result.

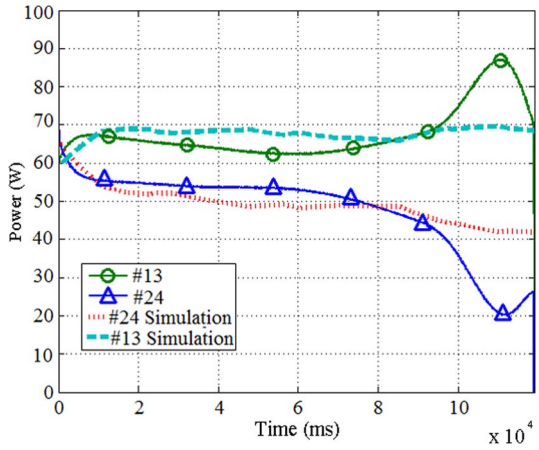

Fig. 21. Cell #13 and #24 simulation result.

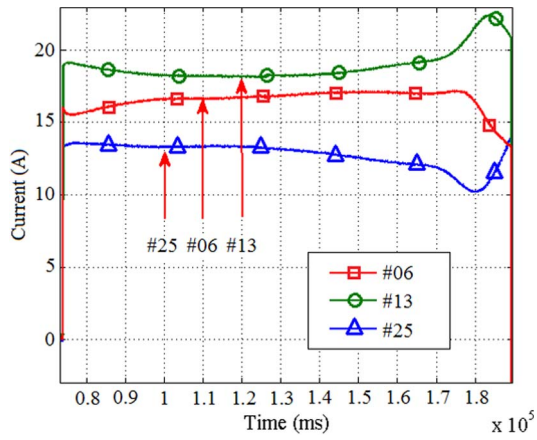

Fig. 22. Group-3 current.

smaller, within 0.4 mΩ. The polarization capacitance C_p and resistance R_p have the similarity at a constant level through the whole discharging process.

With the aforementioned identified parameters, we build the dynamic lumped parameter model of the battery pack with two cells in parallel by using MATLAB/Simulink, as shown in Fig. 19.

The simulation results of Groups 1 and 2 at 1C rate are shown in Figs. 20 and 21, respectively. The simulated current matches the measurement data well during most of the discharging process, except when SOC is approaching zero. The reason is that the OCV and other internal parameters vary very rapidly near the end of the discharging process. The HPPC test data, which are used to identify parameters, only covers 10%–100% SOC. The derived parameters in 0%–10% SOC are accurate enough.

B. Three and Four Cells in Parallel

As the number of cells in parallel increases, the average difference between each cell is decreased. The discharge current of Groups 3 and 4 are shown in Figs. 22 and 23, respectively. The capacity difference between the highest and the lowest still remains around 10 Ah, which is the same as Group 2. With 3-Ah capacity difference between each cell in Group 4, the

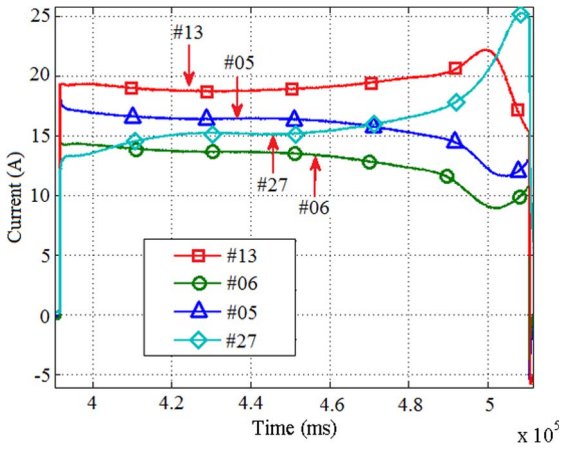

Fig. 23. Group-4 current.

discharging current difference is around 2 A. The distribution shows that each cell's corresponding current is proportional to cell capacity during most of the discharging procedure, except when SOC is approaching zero.

Based on the data comparison between Group 2 and Groups 3 and 4, we conclude that, with more cells in parallel, the current difference is reduced. The current difference at the discharging terminal stage is lower also. These indicate that the battery operation range and lifetime could be prolonged by using more cells in parallel by reducing the probability of inconsistency phenomenon.

C. Discussion

From the aforementioned results and analysis, the cell inconsistency has strong relationship with ohmic resistance, polarization effect, capacity, temperature, SOC, and battery degradation level. The accumulated difference of polarization voltage, parameters, and SOC can jointly affect the current distribution. We can use the SOC difference of each cell in parallel to evaluate the cell inconsistency problem of battery packs.

The battery cells in parallel connection have the characteristic of automatic voltage equilibrium. However, the current and operation SOC range of individual cells may be still different. It means that, when we choose more cells in parallel, the probability of inconsistency phenomenon can be somehow reduced. However, this phenomenon will still exist and could be worse after a long time of operation. The poor cell in the parallel connection will force the better cell to discharge at a much higher current and generate more heat. The consequence is that the overall performance of the cells in parallel may decrease. In EVs, to use cells with small capacity (e.g., 18 650, 26 650 format, 2–5 Ah) in parallel will cause more uncertainty in the system compared with those using single large format battery cells (pouch cell, 20–60 Ah).

Based on the statistical data of cell inconsistency, it is possible to develop some optimization design methods to increase the reliability of battery packs. For example, with maximum 20% degradation difference and two cells in parallel, the cell of a battery pack has the chance to operate at the current 40% higher than normal situation, which increases the heat and severely reduces the reliability of the whole battery pack. When three cells are in parallel, this possibility can be significantly reduced. However, the cost is also increased. In general, to find the best design, which is able to balance the cost, performance, and reliability of battery pack, the statistical data of cell inconsistency is one essential information necessary to know.

V. Conclusion

This paper has mainly studied the characteristics of battery packs formed by lithium-ion cells with different degradation levels in parallel for EV applications. Through various experimental tests and simulations, the characteristics of parallel-connected battery packs have been analyzed and discussed. Cells with different degradation levels in parallel can lead to the accelerated degradation process. The cell inconsistency problem could become worse. To design battery packs and ensure the safe operation, the information and knowledge of cell inconsistency is necessary. However, as the first attempts in modeling of the parallel-connected battery pack, the accuracy is not good enough. The accurate modeling considering cell impedance and connector resistance is our ongoing research goal.

References

[1] C. Mi, A. Masrur, and D. W. Gao, *Hybrid Electric Vehicles: Principles and Applications With Practical Perspectives*. Hoboken, NJ, USA: Wiley, 2011.

[2] R. Xiong, F. Sun, X. Gong, and H. He, "Adaptive state of charge estimator for lithium-ion cells series battery pack in electric vehicles," *J. Power Sources*, vol. 242, pp. 699–713, Nov. 2013.

[3] R. Xiong, X. Gong, C. C. Mi, and F. Sun, "A robust state-of-charge estimator for multiple types of lithium-ion batteries using adaptive extended Kalman filter," *J. Power Sources*, vol. 243, pp. 805–816, Dec. 2012.

[4] S. Li, C. Mi, and M. Zhang, "A high-efficiency active battery-balancing circuit using multiwinding transformer," *IEEE Trans. Ind. Appl.*, vol. 49, no. 1, pp. 198–207, Jan./Feb. 2013.

[5] D. Bortis, J. Biela, and J. W. Kolar, "Active gate control for current balancing in parallel connected IGBT modules in solid state modulators," in *Proc. 16th IEEE Int. Pulsed Power Conf.*, Jun. 17–22, 2007, vol. 2, pp. 1323–1326.

[6] H. Rahimi-Eichi, U. Ojha, F. Baronti, and M. Chow, "Battery management system: An overview of its application in the smart grid and electric vehicles," *IEEE Ind. Electron. Mag.*, vol. 7, no. 2, pp. 4–16, Jun. 2013.

[7] I. Bloom *et al.*, "An accelerated calendar and cycle life study of Li-ion cells," *J. Power Sources*, vol. 101, no. 2, pp. 238–247, Oct. 2001.

[8] K. E. Aifantis, S. A. Hackney, and R. Vasant Kumar, *High Energy Density Lithium Batteries: Materials, Engineering, Applications*, 1st ed. Hoboken, NY, USA: Wiley, Jun. 8, 2010.

[9] U.S. Department of Energy Vehicle Technologies Program, Battery Test Manual For Plug-In Hybrid Electric Vehicles, Revision 0, Dec. 2010. [Online]. Available: http://avt.inel.gov/battery/pdf/PLUG_IN_HYBRID_Manual%20Rev%202.pdf

[10] S. Piller, M. Perrin, and A. Jossen, "Methods for state-of-charge determination and their applications," *J. Power Sources*, vol. 96, no. 1, pp. 113–120, Jun. 2001.

[11] U.S. Department of Energy, Idaho National Laboratory, 2011 Nissan Leaf—VIN 0356 Advanced Vehicle Testing—Beginning-of-Test Battery Testing Results. [Online]. Available: http://www1.eere.energy.gov/vehiclesandfuels/avta/pdfs/fsev/battery_leaf_0356.pdf

[12] U.S. Department of Energy, Idaho National Laboratory, 2013 Chevrolet Volt Advanced Vehicle Testing—Beginning-of-Test Battery Testing Results. [Online]. Available: http://avt.inel.gov/pdf/EREV/fact2013chevroletvolt.pdf

[13] E. Barsoukov and J. Ross Macdonald, *Impedance Spectroscopy: Theory, Experiment, and Applications*, 2nd ed. Hoboken, NJ, USA: Wiley, 2005.

Xianzhi Gong (S'10) received the B.S. degree in electrical engineering and automation from the Nanjing University of Aeronautics and Astronautics, Nanjing, China, in 2009 and the M.S. degree in electrical engineering from the University of New Haven, West Haven, CT, USA, in 2011. He is currently working toward the Ph.D. degree in automotive systems engineering at the Graduate Automotive Technology Education (GATE) Center for Electric Drive Transportation, University of Michigan-Dearborn, Dearborn, MI, USA. His current research interests include battery management, renewable energy, and power electronics.

Rui Xiong (S'12–M'14) received the M.Sc. degree in vehicle engineering and the Ph.D. degree in mechanical engineering from Beijing Institute of Technology, Beijing, China, in 2010 and 2014, respectively. From 2013 to 2014, he was an exchange Ph.D. student with the Department of Electrical and Computer Engineering, University of Michigan, Dearborn, MI, USA.

Since 2014, he has been an Associate Professor with the Department of Vehicle Engineering, School of Mechanical Engineering, Beijing Institute of Technology. He has been invited to deliver speeches and participate on panels for conferences and seminars. He has served as a Reviewer for many journals and conferences. He has more than 40 technical publications, including 33 peer-reviewed journals. He is a holder of two patents. His research interests include system identification, state estimation, adaptive and optimal control, and their applications in areas of electrical and hybrid vehicles, energy storage systems, and smart grid.

Dr. Xiong received the Excellent Master Dissertation and Excellent Doctoral Dissertation from Beijing Institute of Technology in 2010 and 2014, respectively. He is currently a Guest Editor for the *Scientific World Journal* for a special issue on modeling, control, and optimization technologies in electric drive vehicles.

Chunting Chris Mi (S'00–A'01–M'01–SM'03–F'12) received the B.S.E.E. and M.S.E.E. degrees from Northwestern Polytechnical University, Xi'an, China, and the Ph.D. degree from the University of Toronto, Toronto, ON, Canada, all in electrical engineering.

He is a Professor of electrical and computer engineering with the University of Michigan-Dearborn, Dearborn, MI, USA, where he is the Director of the newly established U.S. Department of Energy (DOE)-funded Graduate Automotive Technology Education (GATE) Center for Electric Drive Transportation. He has conducted extensive research and has published more than 100 journal papers. His research interests include electric drives, power electronics, electric machines, renewable-energy systems, and electrical and hybrid vehicles.

Dr. Mi is an Area Editor of the IEEE TRANSACTIONS ON VEHICULAR TECHNOLOGY, an Associate Editor of the IEEE TRANSACTIONS ON POWER ELECTRONICS, and an Associate Editor of the IEEE TRANSACTIONS ON INDUSTRY APPLICATIONS. He served as the Topic Chair for the 2011 IEEE International Future Energy Challenge and the General Chair for the 2013 IEEE International Future Energy Challenge. He is a Distinguished Lecturer of the IEEE Vehicular Technology Society (VTS). He is also the General Co-Chair of the IEEE Workshop on Wireless Power Transfer (WPT) sponsored by the IEEE Power Electronics Society (PELS), IEEE Industry Applications Society (IAS), IEEE Industrial Electronics Society (IES), VTS, IEEE Magnetics Society, and IEEE Power and Energy Society (PES); a Guest Editor-in-Chief of the IEEE TRANSACTIONS ON POWER ELECTRONICS—SPECIAL ISSUE ON WPT; a Guest Editor-in-Chief of the IEEE JOURNAL OF EMERGING AND SELECTED TOPICS IN POWER ELECTRONICS—SPECIAL ISSUE ON WPT; and a Steering Committee Member of the IEEE Transportation Electrification Conference (ITEC-Asian). He is the Program Chair for the 2014 IEEE International Electric Vehicle Conference to be held in Florence, Italy, December 17–19, 2014. He is also the Chair for the IEEE Future Direction's Transportation Electrification Initiative e-Learning Committee.